Published in final edited form as:
Dev Neurobiol. 2009 August ; 69(9): 583–602. doi:10.1002/dneu.20728.

A critical step for postsynaptic F-actin organization: Regulation of Baz/Par-3 localization by aPKC and PTEN

Preethi Ramachandran, **Romina Barria**, **James Ashley**, and **Vivian Budnik***
Department of Neurobiology, University of Massachusetts Medical School, Worcester MA

Abstract

Actin remodeling has emerged as a critical process during synapse development and plasticity. Thus, understanding the regulatory mechanisms controlling actin organization at synapses is exceedingly important. Here we used the highly plastic *Drosophila* neuromuscular junction (NMJ) to understand mechanisms of actin remodeling at postsynaptic sites. Previous studies have suggested that the actiinding proteins Spectrin and Coracle play a critical role in NMJ development and the anchoring of glutamate receptors most likely through actin regulation. Here we show that an additional determinant of actin organization at the postsynaptic region is the PDZ protein Baz/Par-3. Decreasing Baz levels in postsynaptic muscles has dramatic consequences for the size of F-actin and spectrin domains at the postsynaptic region. In turn, proper localization of Baz at this site depends on both phosphorylation and dephosphorylation events. Baz phosphorylation by its binding partner, atypical Protein Kinase C (aPKC), is required for normal Baz targeting to the postsynaptic region. However, the retention of Baz at this site depends on its dephosphorylation mediated by the lipid and protein phosphatase PTEN. Misregulation of the phosphorylation state of Baz by genetic alterations in PTEN or aPKC activity has detrimental consequences for postsynaptic F-actin and spectrin localization, synaptic growth, and receptor localization. Our results provide a novel mechanism of postsynaptic actin regulation through Baz, governed by the antagonistic actions of aPKC and PTEN. Given the conservation of these proteins from worms to mammals, these results are likely to provide new insight into actin organization pathways.

Keywords

Drosophila; synaptic plasticity; neuromuscular junction; actin; trafficking

INTRODUCTION

Reorganization of the actin cytoskeleton plays pivotal roles during the establishment of cell polarity (Wodarz, 2002) and the formation of cellular junctions (Chen and Macara, 2005). In the nervous system, actin remodeling underlies axon pathfinding, synaptogenesis, and synaptic plasticity (Meng et al., 2003; Kalil and Dent, 2005). However, the underlying processes and pathways that regulate actin organization are still poorly understood.

A central property of synapses is their ability to undergo structural and functional changes, such as those occurring during learning and memory (Matsuzaki et al., 2004; Alvarez and Sabatini, 2007). These changes are known to be accompanied by modifications in the actin cytoskeleton (Dillon and Goda, 2005; Lynch et al., 2007). For example, synaptic plasticity

Corresponding author: Vivian Budnik, Department of Neurobiology, University of Massachusetts Medical School, Aaron Lazare Medical Research building, 364 Plantation St., Worcester, MA 01605-2324, USA, Tel. (508) 856-4415, Fax (508) 856-6636, vivian.budnik@umassmed.edu.

in the mammalian brain is accompanied by structural changes in dendritic spines, which involve actin-based cytoskeletal dynamics (Tada and Sheng, 2006).

An important regulator of actin and microtubule cytoskeleton is a conserved cassette of proteins, the Par-3/Par-6/aPKC complex. This complex is essential for the establishment of oocyte and epithelial cell polarity in flies, worms, and mammals (Watts et al., 1996; Lin et al., 2000; Cox et al., 2001; Benton and St Johnston, 2003), and the formation and maintenance of actin-based cell junctions in mammals (Ohno, 2001; Hirose et al., 2002; Chen and Macara, 2005; Munro, 2006). Par-3 and Par-6 are PDZ proteins that bind to and inhibit or activate atypical Protein Kinase C (aPKC) respectively as indicated by studies in primary cell cultures (Lin et al., 2000; Ohno, 2001). These studies also suggest that binding of the small G-proteins, Rac1 or Cdc42, to Par-6 activates aPKC, which in turn phosphorylates Par-3. This phosphorylation leads to the dissociation of Par-3 from aPKC and lifts the inhibition imposed by Par-3 on aPKC kinase activity (Nagai-Tamai et al., 2002). Additionally, the phosphorylation of Par-3 has been implicated in its localization and in modulating actin organization in mammalian epithelial cells (Izumi et al., 1998; Chen and Macara, 2005), but this role is poorly understood.

In the mammalian nervous system, this complex is also involved in establishing neuronal cell polarity (Shi et al., 2003) and in myelination (Chan et al., 2006). Alterations in aPKC activity are associated with defects in synaptic and behavioral plasticity in both mammals and flies (Drier et al., 2002; Pastalkova et al., 2006). At the fly neuromuscular junction (NMJ), aPKC regulates the dynamics of microtubules at presynaptic compartments, and actin-microtubule boundaries at postsynaptic sites, and this regulation is important for synaptic growth, glutamate receptor localization, and normal synaptic function (Ruiz-Canada et al., 2004). However, the exact molecular mechanisms by which aPKC influences postsynaptic actin organization has remained unresolved.

Previous studies have implicated the actin-binding proteins Spectrin and the Band 4.1 homolog Coracle in the regulation of NMJ development and clustering of glutamate receptors (GluR) (Chen et al., 2005; Pielage et al., 2005; Pielage et al., 2006). Here we report that the size of postsynaptic F-actin and spectrin domains also depends on the localization of Baz at the postsynaptic region. In turn, normal Baz localization at the F-actin/spectrin rich area depends on its phosphorylation state. Baz phosphorylation by aPKC allows the translocation of Baz from the muscle cortex to the postsynaptic area. However, a stable localization of Baz at this postsynaptic area requires its dephosphorylation by the lipid and protein phosphatase PTEN, which has also been demonstrated to interact with and is recruited by Baz during the establishment of photoreceptor polarity in flies (von Stein et al., 2005; Pinal et al., 2006). Thus, our results provide a novel molecular mechanism by which postsynaptic F-actin organization is regulated by the phosphorylation state of Baz through the opposing actions of aPKC and PTEN.

MATERIALS AND METHODS

Fly strains

Flies were reared at 25 °C in standard media unless otherwise specified. The following strains were used: wild type (Canton-S), baz^{815-8} (Benton and St Johnston, 2003) (referred to as *baz* mutants in the text), $pten^{dj189FRT40A}$ (Gao et al., 2000) (referred to as *pten* mutant in the text), and $spec^{em6}$ (Dubreuil et al., 2000). We also used the UAS strains UAS-Baz RNAi-1 (see below for generation of this strain), UAS-Baz RNAi (VDRC; referred here to as UAS-Baz-RNAi-2), UAS-PTEN RNAi (Bloomington Stock Center), UAS-aPKC RNAi (see below for generation of this strain), UAS-ϐ-spectrin RNAi (Pielage et al., 2006), UAS-PKM (Drier et al., 2002), and UAS-Baz-GFP (Benton and St Johnston, 2003). To express

transgenes in muscles we used the C57 and BG487 Gal4 strains (Budnik et al., 1996). RNAi crosses were raised at 29° C unless otherwise specified.

Generation of RNAi strains

The aPKC-RNAi transgene was designed against exons 6 and 7 of the *dapkc* genomic region. The Baz-RNAi transgene was designed against exons 3 and 4 of the *baz* genomic region. RNAi constructs were made as in (Kalidas and Smith, 2002). Transgenes were subcloned into the pUAST vector and sent for germ-line transformation to Genetic Services Inc. (Cambridge, MA).

Immunocytochemistry

Body wall muscles from third instar larvae were dissected in Ca^{++}-free saline (Jan and Jan, 1976) and fixed for 30 minutes with 4% paraformaldehyde or 15 min with non-alcoholic Bouin's. Anti-Baz (Wodarz et al., 2000) (1:500), anti-PTEN (1:200; see below), anti-phospho-Baz (1:100; see below), anti-α-spectrin (1:30; Developmental Studies Hybridoma Bank [DSHB]), anti-GluRIIA (1:10; DSHB), anti-GluRIIB and anti-GluRIII (Marrus et al., 2004) (1:500 and 1:200 respectively), anti-DLG_{PDZ} (Koh et al., 1999) (1:20,000), and anti-Scribble (Roche et al., 2002) (1:1000), anti-aPKC (1:1000, Sigma, Santa Cruz, CA), Texas Red or Cy5-conjugated anti-HRP (1:200; Jackson Immunoresearch, West grove, PA) were used as primary antibodies. Postsynaptic and muscle actin was labeled using rhodamine-conjugated phalloidin (1:50–1:100; Molecular Probes). Glutamate receptor staining was performed with an additional round of amplification with anti-FITC (1:800; Sigma, Santa Cruz, CA). As secondary antibodies, FITC-, TxRed-, and Alexa 647-conjugated antibodies (Jackson Immunoresearch, West grove, PA) were used at 1:200.

Generation of the PTEN and Phospho-Baz antibodies

The affinity purified phospho-Baz antibody was raised in rabbits against the peptide CLGRRSISEK with the phosphorylation on the first serine residue (CLGRRpSISEK) by Biosource (also known as QCB; Hopkinton, MA). Affinity purified antibodies against PTEN were raised against two different peptides, CIRNVVSKKRIRYKEKGYD and CISVLHDSATENAKPDRLK, which were coinjected in rabbits by QCB. The specificity of the antibodies was tested by expressing specific RNAi transgenes in muscles and with transfected S2 cells using both immunocytochemistry as well as Western blot analysis.

Confocal microscopy and morphological quantification

Images were acquired using a Zeiss (Oberkochen, Germany) confocal microscope using a 63X objective (1.4 numerical aperture). For comparison between genotypes, confocal stacks were collected from samples that were processed simultaneously and imaged using identical confocal acquisition parameters. Quantification of fluorescence signal intensity was performed by volumetric measurements of the raw data through confocal stacks using Volocity 4.0 Software (Improvision, Waltham, MA). For measurement of postsynaptic volume (V) and intensity (I) single boutons were selected and analyzed as three-dimensional volumes in Volocity. The labeled region around the boutons was segmented by intensity thresholding based on the difference in the intensities at the NMJ vs background intensity. Volume and fluorescence intensity represent the sum of the volumes or intensities of each of the voxels that fell above the threshold value. Presynaptic volume or intensity was measured by calculating the volume or intensity occupied by the label of interest that overlapped with the volume occupied by the anti-HRP label (presynaptic bouton volume). To obtain postsynaptic volume or intensity, the anti-HRP volume was subtracted from the total volume or intensity. Postsynaptic volumes and intensities were expressed as $V_{\text{post-vol or int}} / V_{\text{bouton}}$. For quantification of phospho-Baz, aPKC, or PTEN signal intensity

in muscles, a specific region of muscle 6 was chosen and the puncta were quantified based on size and intensity. Once puncta were segmented, measurements were run for average intensity and size. For GluRIIA, GluRIIB and GluRIII quantification, the volume, mean intensity, and total intensity of individual clusters were calculated using Volocity software. Data were normalized to wild type samples. For F-actin, confocal imaging and quantification was done at muscle 12/13 where the distance between postsynaptic F-actin and the F-actin within the contractile apparatus is relatively large (see Fig. 1C), thus allowing the acquisition of images of NMJ F-actin without interference from the strong myofibril background. All other quantifications were done at muscles 6/7. For determination of the number of type I boutons, body wall muscle preparations were double stained with anti-HRP and anti-Dlg. Measurements were taken from muscles 6 and 7, abdominal segment 3. In all experiments, quantifications of mutant phenotypes were normalized to wild type control samples dissected and imaged using the confocal microscope in the same experimental session. For statistical analysis, unpaired Student's t-tests were run for comparisons between the experimental samples and the wild type controls, which were processed simultaneously. If the variance between the samples was significant, an unpaired t-test with Welch's correction (Frank and Althoen, 1994) was performed. Numbers in histograms represent mean ± SEM. *=$p< 0.05$, **=$p< 0.001$, ***=$p< 0.0001$.

Western Blots

Full-length Baz, PKM and dPTEN2 cDNAs were subcloned into the pAcV5.1/HisA or -B vector (Invitrogen, Carlsbad, CA) for transfection into *Drosophila* Schneider-2 (S2) cells. Mutations in the dPTEN2 construct eliminating the lipid (G137E) and protein (C132A) phosphatase activity were carried out using the QuikChange II Site-Directed Mutagenesis Kit (Strategene, La Jolla, CA). Cell cultures were centrifuged at 1000g × 5min, the pellet lysed in lysis buffer (20mM Tris HCL pH 7.5, 150mM NaCl, 1mM EDTA, 1mM EGTA, 1% NP-40, 25μM MG132, protease inhibitor cocktail (Thomas et al., 1997), and phosphatase inhibitor I and II cocktail (Calbiochem, San Diego, CA) for the kinase assay, and without the phosphatase inhibitor for the PTEN dephosphorylation assay, and then boiled with sample buffer containing 10% DTT and 5% β-mercaptoethanol. Proteins were separated on 5% SDS PAGE gels, transferred onto a PVDF or nitrocellulose membrane and sequentially immunoblotted with anti-phospho-Baz (1:5000), anti-Baz (1:2000) and anti-α-spectrin (1:1000). For the lambda phosphatase assay, proteins were transferred onto a nitrocellulose membrane and incubated in Tris Buffered Saline (TBS) containing 1% BSA, 0.1% Triton X-100, 2 mM $MnCl_2$ and 400 μl/ml of lambda phosphatase (Upstate, Lake Placid, NY) for 1 hour at room temperature, following which they were washed with TBS with 0.1% Tween20 and sequentially probed with anti-phospho-Baz (1:5000) and anti-Baz (1:2000). Bands were visualized by chemoluminiscence methods (Amersham, Piscataway, NJ). Normalized P-Baz/Baz band intensities were measured using Image J. After adjusting for loading (spectrin) control and subtracting the background provided by non-transfected controls, values were normalized to Baz or P-Baz from Baz-transfected cells, and the ratio P-Baz/Baz calculated.

Transmission Electron Microscopy

Body wall muscles were prepared for TEM as in (Jia et al., 1993; Packard et al., 2002). Analysis of SSR thickness was done as (Budnik et al., 1996). For analysis of the distance between the outer SSR boundary and the myofibrils at muscle 12, 15 boutons from 3 preparations were used. Comparisons of SSR thickness in wild type and aPKC-RNAi-post animals was done from 3 wild type (9 boutons measured at the bouton midline) and 3 aPKC-RNAi-post animals (6 boutons measured at the bouton midline). For statistical analysis, unpaired Student's t-tests were run for comparisons between the experimental samples and the wild type control.

Electrophysiology

Larval body wall muscle voltage recordings were performed as in (Ashley et al., 2005). Briefly, recordings were collected from muscle 6 of wandering 3rd instar larvae, and only those muscles with resting potentials between −60 mV to −63 mV wereanalyzed. Larva were dissected in HL-3 saline (Stewart et al., 1994) containing 0.3 mM Ca^{2+} and recorded in HL-3 saline containing 0.5 mMCa^{2+}. Recordings collected using an Axoclamp 2A (Molecular Devices, Union City, CA) were digitized usingan Instrutech (Port Washington, NY) ITC-16 computer interface, processed using Pulse software (HEKA Electronik, Lambrecht/Pfalz, Germany) and measured using Mini Analysis software (Synaptosoft, Decatur, GA.). For statistical analysis, unpaired Student's t-tests were run for comparisons between the experimental samples and the wild type controls.

RESULTS

aPKC activity regulates the organization of the postsynaptic F-actin and spectrin area

The *Drosophila* larval NMJ is innervated by glutamatergic motorneurons that branch over the body wall muscles in a stereotypic fashion. These terminals are composed of synaptic boutons containing synaptic vesicles and vesicle release sites (Prokop, 2006). Synaptic boutons at the NMJ are completely surrounded by the muscle membrane, which forms a highly folded structure, the subsynaptic reticulum (SSR) (Fig. 1A, C, G). This specialized postsynaptic region is highly enriched in F-actin, as determined by labeling with fluorescently labeled phalloidin (Coyle et al., 2004; Chen et al., 2005; Nunes et al., 2006) (Fig. 1B, arrowhead), and the actin-binding protein spectrin (Ruiz-Canada et al., 2004; Pielage et al., 2006). Three-dimensional reconstructions of confocal Z-series using Volocity software showed that this postsynaptic F-actin domain appeared separate from the muscle contractile apparatus (Fig. 1B, two-way arrow; distance is 2.5±0.16 μm; N=23 arbors; Suppl. Movie 1). This was also supported by visualization of the terminals at muscle 12 by electron microscopy, showing that myofibrils are separated from the SSR (Fig. 1C–F, G; red two-way arrows; distance is 1.6± 0.4, N=15 boutons). Beyond this F-actin/spectrin-rich postsynaptic area there is a microtubule network at the muscle cortex which radiates from the nuclei, and which terminates at the boundary of the F-actin/spectrin-rich area (Ruiz-Canada et al., 2004) (Fig. 1A). Previous studies demonstrated that aPKC is localized both inside synaptic boutons and at the microtubule-rich cortical muscle area, but it is absent from the postsynaptic F-actin/spectrin regions (Ruiz-Canada et al., 2004). Decrease in aPKC protein levels led to a disruption in the presynaptic microtubule cytoskeleton by reducing the interaction between microtubules and the presynaptic MAP1B-related protein Futsch, while increase in aPKC activity increased this interaction (Ruiz-Canada et al., 2004). Surprisingly however, mutations in *dapkc* altered the extent of the postsynaptic spectrin region. This observation was surprising, as aPKC is absent from this area (Ruiz-Canada et al., 2004). As an initial attempt to understand the mechanisms by which aPKC could regulate the postsynaptic spectrin region, we first determined if the decrease in spectrin levels upon decreasing aPKC activity was accompanied by changes in the postsynaptic F-actin domain. We used rhodamine-conjugated phalloidin to label F-actin, and expressed aPKC-RNAi only in the muscles, which reduced aPKC levels in muscle by 50–60% (Suppl. Fig. 1A, B). As previously reported, F-actin was found enriched around synaptic boutons (Coyle et al., 2004; Chen et al., 2005; Nunes et al., 2006), in exact colocalization with α-spectrin (Fig. 2A, D; arrows) and showed a diffuse meshwork-like appearance (which here is referred to as "F-actin meshwork"). Reducing aPKC levels in muscles alone by expressing aPKC-RNAi using the muscle specific Gal4 driver C57 (Budnik et al., 1996) (aPKC-RNAi-post), was sufficient to substantially reduce spectrin around synaptic boutons (Fig. 2B1, B3 arrows; H, I) and this was accompanied by a similar reduction in postsynaptic F-actin (Fig. 2B2–3, E arrows; H, I). Thus, spectrin is exactly localized to the F-actin-rich postsynaptic area, and decreasing

aPKC activity leads to a concomitant reduction in both F-actin and spectrin. This reduction in F-actin and spectrin was not due to changes in the extent of the SSR, as demonstrated by electron microscopy (Suppl. Fig. 2A) and staining with the SSR markers DLG and Scrib (Suppl. Fig. 2B, C).

The decrease in F-actin at the postsynaptic region observed upon aPKC downregulation might result from a reduction in spectrin, as spectrin is known to crosslink F-actin microfilaments and facilitate the formation of a network/meshwork-like arrangement (Cohen et al., 1980). If this was the case, then downregulation of spectrin alone should mimic the phenotype observed upon expressing aPKC-RNAi in postsynaptic muscles. This possibility was examined in both *β-spectrin* mutants (Featherstone et al., 2001) and by expressing a ϐ-spectrin-RNAi (ϐ-spec-RNAi; (Pielage et al., 2006)) in muscles. Both α– and ϐ-spectrin were virtually eliminated in heterozygote *β-spec*^{em6}/+ (Fig. 2C1) (Featherstone et al., 2001) and upon expressing ϐ-spectrin RNAi in body wall muscles (Suppl. Fig. 1C, D) (Pielage et al., 2006). This virtual elimination of α- and ϐ-spectrin in *β-spec*^{em6}/+ heterozygous animals is likely due to a dominant-negative effect of a truncated ϐ-spectrin product generated in the *β-spec*^{em6} mutation (Featherstone et al., 2001). In both the *β-spec*^{em6}/+ heterozygotes as well as the ϐ-Spectrin-RNAi-post, F-actin lost its meshwork-like organization around synaptic boutons and became organized into short and thin wisps/spikes (Fig. 2C2–3, F, G). These wisps/spikes appeared quite different from the F-actin phenotype observed upon downregulation of aPKC in muscles. Similar F-actin wisps have previously been shown to be associated with the loss of Fodrin, a non-erythrocyte type spectrin (Sato et al., 2004). Thus while loss of spectrin changes the configuration of postsynaptic F-actin from meshwork-like to wisps, aPKC downregulation influences the size of the postsynaptic F-actin/spectrin domain.

The aPKC substrate Baz regulates the size of the postsynaptic F-actin-rich area

The above results suggest that spectrin is critical for postsynaptic F-actin organization, but does not seem to be the sole determinant. To search for additional regulators of F-actin and spectrin that might underlie the effects of aPKC at the postsynaptic region, we focused on a known aPKC substrate, Baz/Par-3, which is also present at the NMJ (Nagai-Tamai et al., 2002; Ruiz-Canada et al., 2004). Baz has been implicated in the formation of actin-based cellular junctions in mammalian epithelial cells (Lin et al., 2000; Munro, 2006). At the larval NMJ, Baz is highly enriched at the postsynaptic F-actin region (Ruiz-Canada et al., 2004), but it is also present in a punctate pattern at microtubule-rich areas (Fig. 3A) where aPKC is localized (Ruiz-Canada et al., 2004). Therefore, we determined if the regulation of postsynaptic F-actin and spectrin by aPKC could involve Baz. Consistent with this view, decreasing aPKC activity in muscle alone, by expressing aPKC-RNAi in muscles resulted in a reduction in Baz localization at the postsynaptic region in exact correspondence with the reduction in F-actin area (Fig. 3B, I). This decrease in Baz, spectrin, and F-actin at the postsynaptic region was quite specific, as it was not accompanied by a significant decrease in the levels or localization of other proteins present at this region, such as the scaffolding proteins DLG and Scrib (Suppl. Fig. 2B, C). Thus, aPKC might regulate postsynaptic F-actin in part through Baz.

The above possibility was examined by determining if downregulating Baz in muscles mimicked the consequences of decreasing aPKC with respect to NMJ structure and localization of synaptic proteins. Null mutations in *baz* result in embryonic lethality due to the role of this protein in establishing cell polarity (Izumi et al., 1998; Lin et al., 2000; Nagai-Tamai et al., 2002). Therefore, in order to downregulate Baz we expressed Baz-RNAi in the muscle using the UAS-Gal4 system. To support the idea that the effects observed were not due to off target RNAi effects, we used two different RNAi lines in which the RNAi was directed against two different regions of the Baz mRNA, as well as Baz-RNAi in

a *baz*/+ heterozygous background. In all of the above genotypes Baz immunoreactivity was significantly decreased (Fig. 3C, D; Suppl. Fig. 3). Further, downregulating *baz* in all of the genotypes resulted in phenotypes that completely overlapped with those observed by aPKC downregulation in muscles. First, the volume and intensity of the spectrin and F-actin rich postsynaptic region was drastically reduced (Fig. 3E–H, J, K). Second, synaptic boutons were significantly reduced in number and had an abnormal morphology as well as a significant increase in volume, similar to aPKC-RNAi-post (Fig. 3L, M). Similar reductions in synaptic bouton number have been observed in other conditions that alter the synaptic cytoskeleton (Pielage et al., 2006; Koch et al., 2008). This reduction in bouton number was not seen in the UAS line or the muscle specific Gal4 line alone showing that these insertions by themselves do not affect NMJ morphology or bouton number (Suppl Fig. 4). Thus, downregulation of *baz* or *dapkc* result in the same phenotypes.

Phospho-Baz is excluded from the F-actin/spectrin rich postsynaptic region

The above results raised a number of important questions. For example, endogenous aPKC is not localized at the postsynaptic F-actin rich area, but rather is present in puncta outside this area (Ruiz-Canada et al., 2004) (see Fig. 1A). Therefore, if aPKC regulates F-actin by phosphorylating Baz, then this event must occur outside the F-actin-rich postsynaptic area. This possibility was addressed by examining the localization of phosphorylated Baz, and the dependency of Baz phosphorylation on aPKC activity. Phospho-specific Baz antibodies were raised against the conserved peptide containing the serine residue (S980 in Baz) known to be phosphorylated by aPKC in mammals and flies (Nagai-Tamai et al., 2002; Benton and St Johnston, 2003). Surprisingly, we found that in postsynaptic muscles phospho-Baz immunoreactivity was present in a punctate pattern in the muscle (Fig. 4A) and was actually excluded from the F-actin/spectrin-rich area (Fig. 4D). In addition phospho-Baz was present inside presynaptic boutons (Fig. 4D). This immunoreactivity was specific and depended on Baz phosphorylation by aPKC as demonstrated by four lines of evidence. First, expressing a constitutively active aPKC form, PKM, in muscles increased the overall size and intensity of the phospho-Baz immunoreactive muscle puncta (Fig. 4B, F). Second, decreasing aPKC levels specifically in muscle by expressing aPKC-RNAi resulted in substantial decrease in the size and intensity of the puncta (Fig. 4E, F). Third preincubating the antibody with the phosphopeptide used as immunogen completely eliminated immunoreactivity (Suppl. Fig. 5A, B). Finally, phospho-Baz immunoreactivity was significantly reduced in *baz*/+; Baz-RNAi-post larvae (Fig. 4C, F).

To determine if endogenous P-Baz puncta in the muscle cortex colocalized with a subset of endogenous Baz puncta, we carried out sequential immunolabeling (incubations: P-Baz primary → wash → FITC-secondary → wash → Baz primary → wash → TxR-secondary → wash), as both anti-P-Baz and anti-Baz antibodies were made in rabbit, precluding the simultaneous double-labeling technique (Fig. 4G). To ensure that the application of the first round of rabbit secondary (FITC-secondary) completely saturated binding sites in the P-Baz antibody, we performed a control, in which samples were incubated with TxR-secondary after the FITC-secondary antibody (incubations: P-Baz primary → wash → FITC-secondary → wash → TxR-secondary → wash) (Fig. 4I). No labeling in the red channel was found under these conditions, demonstrating complete saturation of the anti-P-Baz antibody binding sites after the FITC-secondary incubation (Fig. 4I2). We found that every P-Baz puncta exactly colocalized with a Baz puncta (Fig. 4G, arrows). However, only a subset of Baz puncta colocalized with P-Baz puncta (Fig. 4G, arrowheads), showing that not every Baz puncta becomes endogenously phosphorylated. This result was confirmed by expressing a GFP-tagged Baz transgene (Baz-GFP) in wild type muscles, which colocalized to a subset of Baz puncta (Suppl. Fig. 6 A; yellow arrowheads). When the Baz-GFP-post samples were double labeled with the P-Baz antibody, we observed a subset of puncta which were positive

for both GFP as well as phospho-Baz immunoreactivity (Suppl. Fig. 6B; yellow arrowheads). To determine if this colocalization was the result of simply random coincidence between puncta in the Baz, P-Baz and GFP channels, we rotated the GFP channel at a 90° angle. If the colocalization was simply coincidence, then this rotation should not affect the number of puncta that are colocalized. However, upon 90° rotation there was little colocalization between the GFP and Baz or P-Baz puncta (Suppl. Fig. 6C, D), demonstrating that Baz-GFP and P-Baz or Baz-GFP and Baz show a true colocalization. Thus, Baz is phosphorylated at S980 by aPKC outside the postsynaptic F-actin/spectrin-rich region, and therefore the Baz protein observed at the postsynaptic F-actin/spectrin-rich area most likely corresponds to **de**phosphorylated Baz.

The ability of aPKC to phosphorylate Baz was also demonstrated in Schneider-2 (S2) cells single or double transfected with aPKC and/or Baz. Baz is endogenously expressed in S2 cells but at low levels, and therefore a very faint phospho-Baz band was observed in untransfected cells (Fig. 4H), most likely due to the activity of endogenous aPKC. Ratiometric comparison of phospho-Baz levels to Baz levels in different lanes showed that cells transfected with Baz alone or with PKM alone showed a weak increase in the intensity of this band (Fig. 4H; Suppl. Fig. 7A). However, this increase was not related to the absolute levels of Baz and was due in part to the presence of endogenous proteins. In contrast, cells transfected with Baz and PKM showed a drastic enhancement (100% increase) in the intensity of the phospho-Baz band (Fig. 4H; Suppl. Fig. 7A). This effect was reversed by treating the Western blots with lambda phosphatase, which eliminated the increase in the P-Baz band levels in Baz and PKM double transfected cells (Fig. 4J).

PTEN is a phosphatase localized at the F-actin rich postsynaptic area and is required for postsynaptic Baz localization

The observations described above, suggest that Baz is phosphorylated by aPKC outside the postsynaptic F-actin/spectrin-rich area. Further, they indicate that Baz protein at the postsynaptic F-actin/spectrin-rich region represents **de**phosphorylated Baz. This raised the question of why a decrease in aPKC activity, which results in a decrease in the phosphorylation of Baz, actually leads to a decrease in Baz at the F-actin/spectrin-rich area. A potential model is that Baz phosphorylation is required for proper transport or targeting of Baz to the F-actin/spectrin-rich area, but that the retention of Baz at this site requires a de-phosphorylation event (Fig. 5A). To test this model, we used a candidate approach to identify the putative phosphatase mediating Baz dephosphorylation.

Recent studies in flies have demonstrated that Baz interacts with the lipid and protein phosphatase PTEN (von Stein et al., 2005; Pinal et al., 2006) and that Baz is required to recruit PTEN to regions of actin remodeling (Pinal et al., 2006). Therefore, an attractive Baz phosphatase candidate was PTEN. Three predictions of our hypothesis (Fig. 5A) are that (1) PTEN should be localized to the F-actin/spectrin-rich postsynaptic area, where **de**phospho-Baz is localized, (2) that mutations in *pten* should decrease the amount of **de**phospho-Baz localized at the F-actin/spectrin-rich region, and (3) that mutations in PTEN should increase the amount of P-Baz at the muscle cortex (outside of the F-actin/spectrin-rich area). To test these predictions we generated an anti-peptide PTEN antibody recognizing all PTEN splice variants (PTEN1-3 (Pinal et al., 2006); Suppl. Fig. 5C, D). As predicted, in wild type larvae, PTEN was highly enriched at the F-actin/spectrin region where it exactly colocalized with Baz as determined by its precise colocalization with F-actin at this area (Fig. 5D, F). The PTEN immunostaining was specific, as expressing PTEN-RNAi, which knocks down all PTEN isoforms, in muscles of wild type (PTEN-RNAi-post) or in a *pten*/+ heterozygous background, resulted in a drastic reduction in both postsynaptic as well as muscle cortical PTEN levels (Fig. 5E, B, C). The *pten* mutant utilized in this study (see methods) has been previously identified as a null allele of *pten* resulting from an F-element insertion that

completely eliminates the phosphatase domain, and which leads to embryonic lethality (Gao et al., 2000). Furthermore, preincubating the antibody with the peptide used as immunogen virtually eliminated immunoreactivity from the muscle cortex (Suppl Fig. 5C, D).

The colocalization between Baz and PTEN, as well as the previously reported interactions between the two proteins placed PTEN as a strong candidate for mediating the dephosphorylation of Baz at the F-actin/spectrin-rich postsynaptic area, and according to our model, for the retention of Baz at this area. Therefore, we next examined if downregulating PTEN would result in changes in the localization of Baz at the peribouton area. As predicted, downregulating PTEN resulted in a drastic reduction of Baz localization at the postsynaptic F-actin rich area (Fig. 6A, B, K) and a similar reduction was observed in both the spectrin (Fig. 6C, D, I, J) as well as the F-actin area (Fig. 6I, J). Other markers of the F-actin/spectrin area, such as DLG and Scrib were not changed (Supp. Fig. 2B, C).

Consistent with our hypothesis, downregulating PTEN in muscles also resulted in a significant increase in muscle P-Baz puncta outside the postsynaptic F-actin rich area (Fig. 6E, F, L). Together, these results provide compelling evidence that PTEN induces the dephosphorylation of Baz at S980, and that phosphorylated Baz is not retained at the postsynaptic region. Interestingly, downregulating Baz also resulted in a decrease in PTEN localization at the peribouton area (Fig. 6G, H) consistent with previous observations in photoreceptor cells that Baz has a role in recruiting PTEN to the membrane (Pinal et al., 2006).

The possibility that PTEN could be involved in dephosphorylating Baz was also tested in S2 cells single or double transfected with Baz and PTEN variants. Given that Baz has been shown to specifically interact with PTEN2 and not with other isoforms of PTEN (von Stein et al., 2005; Pinal et al., 2006), wild type and mutated PTEN2 cDNAs were used to transfect S2 cells. Transfection with Baz showed that Baz was endogenously phosphorylated in S2 cells as revealed with the P-Baz antibody (Fig. 6M; Suppl. Fig. 7B). In contrast, in cells double transfected with Baz and PTEN2, the level of P-Baz phosphorylation was drastically reduced (Fig. 6M; Suppl. Fig. 7B), demonstrating that PTEN is involved in the dephosphorylation of Baz. Additionally, mutating the PDZ binding domain of PTEN2, responsible for its interaction with PDZ2-3 of Baz, completely prevented this dephosphorylation (Fig. 6M; Suppl. Fig. 7B), suggesting that the direct interaction between Baz and PTEN2 is required for Baz dephosphorylation. This observation further raises the possibility that PTEN might directly dephosphorylate P-Baz.

PTEN has both lipid and protein phosphatase enzymatic activity (Lee et al., 1999). Therefore, we next tested which of these activities was required for the dephosphorylation of P-Baz. In particular, we generated a PTEN2 variant, $PTEN2^{C132A}$, in which a conserved cysteine (C124 in mammals, C132 in flies) is required for both protein phosphatase and lipid phosphatase activity (Cai et al., 2005), was mutated to alanine. In addition, we generated a PTEN2 variant, $PTEN2^{G137E}$, in which a conserved glycine (G129 in mammals and G137 in flies), required for the lipid phosphatase activity alone (Cai et al., 2005), was mutated to glutamate. As expected, blocking lipid phosphatase activity in $PTEN2^{G137E}$, did not affect the ability of PTEN2 to dephosphorylate P-Baz (Fig. 6M; Suppl. Fig. 7B). In contrast, blocking both the protein and lipid phosphatase activity in $PTEN2^{C132A}$ completely blocked P-Baz dephosphorylation (Fig. 6M; Suppl. Fig. 7B). Together with the observation that normal localization of Baz at the peribouton area depends on PTEN, that PTEN colocalizes with dephospho-Baz, the above results are consistent with the model that dephosphorylation of Baz by PTEN is required to retain Baz at the postsynaptic region, that Baz dephosphorylation requires its direct interaction with PTEN and depends on the protein phosphatase activity of PTEN.

Downregulation of PTEN partially mimics mutations in *baz* and both genes interact

In addition to the changes in Baz, Spec, and F-actin upon PTEN downregulation, which were identical to those observed by reducing Baz or aPKC in muscles, we found that other common phenotypes were also present. For example, in both *pten/+*; PTEN-RNAi-post or PTEN-RNAi-post alone there was a significant decrease in the number of synaptic boutons (Fig. 7A). In addition, bouton volume was significantly increased in PTEN-RNAi post larvae (Fig. 7B).

To further support the notion that PTEN functions in the same developmental pathway at the NMJ as Baz, we used a classical genetic test in null mutant transheterozygotes (Anholt and Mackay, 2004; Greenspan, 2006; Pawson et al., 2008). Heterozygote *pten/+* or *baz/+* larvae had NMJs that were indistinguishable from wild type (Fig. 7C). However, the transheterozygotes displayed a significant reduction in the number of synaptic boutons, strongly suggesting the presence of genetic interactions between *pten* and *baz* (expected reduction in synaptic bouton number for purely additive interactions is 19% reduction vs. 30% reduction found in the transheterozygote; Fig. 7C).

Downregulation of aPKC, PTEN and Baz have similar effects on synaptic transmission and glutamate receptor localization

Previous studies demonstrated that mutations in aPKC led to a drastic increase in glutamate receptor IIA (GluRIIA) levels and a substantial increase in the amplitude of spontaneous events (Ruiz-Canada et al., 2004). Therefore we next examined if GluR localization and synaptic transmission was similarly altered by down regulating *baz* and *pten* postsynaptically. We found that the volume, mean intensity, and total intensity of GluRIIA clusters were significantly increased in *baz/+;* Baz-RNAi-post and *pten/+*; PTEN-RNAi-post NMJs (Fig. 8A, C, D, G), and this increase was similar to that observed by downregulating aPKC in muscle cells (Fig. 8B, G). In addition to the increase in GluRIIA, other glutamate receptors such as GluRIIB and GluRIII were also increased (Suppl. Fig. 8A, B). The increase in GluR cluster size and intensity was consistent with the observation that the amplitude of miniature excitatory junctional potentials was also increased in all three mutants (Fig. 8F, H).

While the changes in mEJP amplitude were similar upon downregulating aPKC, Baz, and PTEN, other functional defects differed among genotypes. For example, the amplitude of nerve evoked excitatory junctional potentials (EJP) was significantly increased when Baz and aPKC were downregulated, no such increase in EJP amplitude was observed upon PTEN downregulation (Fig. 8E, J). In addition, while there was a significant increase in the frequency of mEJPs upon dowregulating Baz and PTEN, no such change was observed in aPKC-RNAi-post (Fig. 8I). Thus, while the distribution of GluRs and mEJP amplitude is likely to operate using a common pathway involving aPKC, Baz and PTEN, there are other functional aspects of synaptic transmission in which the function of each protein might be independent. Alternatively, compensatory mechanisms observed at these synapses (DiAntonio et al., 1999) might be activated to different extents in the three mutant backgrounds.

DISCUSSION

Previous studies have implicated the actin-binding proteins spectrin and Coracle in NMJ development and in the selective clustering of GluR subunits most likely through the regulation of pre- and postsynaptic F-actin (Chen et al., 2005; Pielage et al., 2006). Here we identify an additional novel mechanism by which postsynaptic F-actin/spectrin is regulated during NMJ expansion. Previously, we reported that the aPKC-Baz-Par-6 complex is present

at the NMJ and that aPKC was required for normal NMJ expansion and presynaptic microtubule stability (Ruiz-Canada et al., 2004). Here, we show that aPKC and Baz in conjunction with the lipid and protein phosphatase PTEN play an additional role in regulating postsynaptic F-actin/spectrin through a novel mechanism. We propose that Baz is required to stabilize the postsynaptic F-actin/spectrin meshwork, and this process involves changes in its phosphorylation state (Fig. 9). Our evidence suggests that proper targeting of Baz to the postsynaptic region requires its phosphorylation by aPKC, but its retention at this region may requires its dephosphorylation by PTEN (Fig. 9).

Several lines of evidence support this model. First, reduction of aPKC, Baz and PTEN levels in the muscles result in a similarly dramatic reduction in postsynaptic F-actin. Second, Baz localization at the postsynaptic F-actin-rich region depends on its phosphorylation state. While phosphorylated Baz is excluded, dephosphorylated Baz is concentrated at this site. Third, aPKC is also excluded from the F-actin-rich region and a decrease in Baz phosphorylation by aPKC results in a decrease in Baz at the F-actin rich area. This suggests that aPKC-dependent phosphorylation of Baz occurs outside the F-actin-rich region and that this phosphorylation may be required for proper targeting but not for retention of Baz at the actin-rich postsynaptic region. Fourth, PTEN colocalizes with dephospho-Baz at the actin-rich postsynaptic region and reducing PTEN levels results in a reduction in Baz at this site, and in an increase in phospho-Baz levels in the surrounding area. Thus, the retention of Baz at the F-actin-rich area requires its dephosphorylation, which is likely mediated through PTEN. Fifth, there is a significant overlap in NMJ phenotypes upon downregulating Baz, aPKC and PTEN, and Baz and PTEN interact genetically suggesting that they might function in the same pathway during NMJ expansion.

Studies in mammalian cells have implicated Par-3 in the maintenance of actin-based junctions, such as the tight junction (Chen and Macara, 2005; Nishimura et al., 2005). Baz is an aPKC substrate, and our studies at the NMJ show that it is in exact colocalization with F-actin. Collectively, this indicates that the effects of aPKC on F-actin/spectrin are mediated most likely through Baz, and that Baz is required for the normal organization of the postsynaptic F-actin/spectrin meshwork. Any reduction in postsynaptic Baz levels as seen by decreasing aPKC, Baz, or PTEN resulted in a decrease in the density and thickness of the postsynaptic F-actin cytoskeleton.

Several potential mechanisms by which Par-3/Baz might regulate F-actin have been suggested, including dephosphorylation of Cofilin through the inhibition of LIM kinase (Chen and Macara, 2006), and regulation of the Rac Guanine nucleotide exchange factor, Tiam1 (Chen and Macara, 2005; Nishimura et al., 2005). Although, *Drosophila* LIMK and Tiam1 are absent from the postsynaptic region (Sone et al., 1997; Eaton and Davis, 2005), Baz might regulate dPIX, another Rho-GEF that is enriched postsynaptically (Parnas et al., 2001) and its downstream effector dPAK (Conder et al., 2007). Another potential mechanism could involve an interaction between the PDZ2 domain of Baz and membrane phospholipids (Wu et al., 2007). By binding to phospholipids, Baz might bring together a number of actin regulators to the membrane to remodel postsynaptic F-actin.

Cell culture studies demonstrate that Par-3 is phosphorylated by aPKC, which results in the dissociation of the two proteins and targeting and stabilization of phospho-Par-3 at sites of tight junction formation (Hirose et al., 2002; Nagai-Tamai et al., 2002). We hypothesize that phosphorylation of Baz at S980 is similarly required to target Baz to the postsynaptic region. We determined that phospho-S980-Baz was distributed in puncta at the muscle cortex, but excluded from the postsynaptic F-actin-rich area. Consistent with previous studies (Nagai-Tamai et al., 2002), altering muscle aPKC levels resulted in the respective increase or decrease in phospho-Baz levels in the muscle. Thus, our immunocytochemical results,

supported by our biochemical assays, strongly validate the idea that Baz is phosphorylated by aPKC in the muscle. To our knowledge, this is the first study to demonstrate the phosphorylation of Baz by aPKC in the context of an intact organism, and during NMJ development. We suggest that, as in mammals, phosphorylation of Baz might disrupt the binding between Baz and aPKC allowing phospho-Baz to be mobilized to the postsynaptic region. However, unlike previous studies which hypothesized that phospho-Par-3 was stabilized at the apical region (Nagai-Tamai et al., 2002), our studies showed that phospho-Baz was absent from the postsynaptic region. Instead, we found that Baz at this region was present in a dephosphorylated state. Thus we postulate that while targeting Baz to the postsynaptic region requires aPKC phosphorylation, its actual retention at this site necessitates its dephosphorylation.

Studies in epithelial cells show that Baz interacts with the lipid and protein phosphatase PTEN through binding between the PDZ2-3 domain of Baz and the PDZ binding motif in PTEN2 (von Stein et al., 2005; Pinal et al., 2006). Further, these studies demonstrated that Baz was required for the recruitment of PTEN to regions of actin remodeling (Pinal et al., 2006). These observations made PTEN a prime candidate for Baz dephosphorylation. Confirming this model, we found that PTEN was colocalized with dephospho-Baz at the postsynaptic region. Moreover, reducing PTEN activity resulted in a decrease in dephospho-Baz at the postsynaptic region and an increase in phospho-Baz in muscle suggesting that PTEN-dependent dephosphorylation of Baz is necessary to retain Baz at the postsynaptic region. Additionally, our biochemical assays indicate that this dephosphorylation requires the PDZ interaction between PTEN and Baz and is mediated by the protein phosphatase activity of PTEN. PTEN has been shown to directly dephosphorylate many different proteins such as FAK kinase (Tamura et al., 1998), but might also function indirectly through the activation of other protein phosphatases (Traweger et al., 2008). Notably, we found that the localization of Baz and PTEN was interdependent for their mutual localization at the postsynaptic region. Consistent with results of previous studies (Pinal et al., 2006), Baz downregulation also decreased postsynaptic PTEN supporting the idea that Baz is required for PTEN localization at postsynaptic sites.

Several studies have implicated PTEN in regulating synaptic structure and function (Fraser et al., 2008), neurotransmitter receptors (Ning et al., 2004; Ji et al., 2006), hippocampal LTD (Wang et al., 2006), neuronal arborization, and social interactions in mice (Kwon et al., 2006). Our studies demonstrate for the first time that PTEN is involved in inducing the dephosphorylation of Baz and the regulation of the postsynaptic F-actin cytoskeleton. Thus, these studies reveal a potential molecular mechanism for PTEN function in the nervous system.

A previous study in embryonic NMJs demonstrated a role for postsynaptic F-actin in the proper clustering of GluRIIA-, but not of GluRIIB-receptors through the fly Band 4.1 homolog, Coracle (Cora), which appears to interact directly with the C-terminal tail of GluRIIA (Chen et al., 2005). In *cora* mutants, GluRIIA-, but not GluRIIB-cluster size and function was reduced (Chen et al., 2005). Pharmacological disruption of F-actin using Lantrunculin mimicked this mutant phenotype, leading the authors to suggest that Cora might function to directly anchor GluRIIA subunits to F-actin (Chen et al., 2005). In our studies and Ruiz-Canada et al (2004) we found that GluRIIA-, GluRIIB-, and GluRIII-cluster volume and intensity was significantly increased upon downregulating either aPKC, Baz, or PTEN, and that this phenotype was accompanied by an increase in the amplitude of mEJPs. However, in our studies the postsynaptic F-actin region was not completely disrupted, but significantly reduced in size. This raises the interesting possibility that beyond anchoring receptors on the postsynaptic membrane, the F-actin and spectrin domain might act as a barrier to the diffusion and clustering of receptors at the postsynaptic area or may

affect the recycling of receptors. In this regard, it is important to note that an increase in GluRIIA, GluRIIB, and GluRIII size was also observed in another study where spectrin was dowregulated exclusively in the larval muscles using RNAi (Pielage et al., 2006). Furthermore, this study also found an increase in the mEJP amplitude upon downregulation of spectrin in the muscle. These studies implicated spectrin in regulating active zone size and spacing, as well as synaptic efficacy. While some of the phenotypes reported upon spectrin elimination in the muscle, were similar to those examined here upon downregulating aPKC, Baz, and PTEN, others were quite different. For example, spectrin elimination resulted in disrupted SSR and abnormal localization of DLG. The loss of SSR, in addition to being a result of disorganized Dlg, as suggested by the study (Pielage et al., 2006), could also be due to a change in postsynaptic F-actin configuration from meshwork to wisps seen in *spec* mutants and ϐ-Spec-RNAi-post. In contrast, we found that the SSR was intact upon expressing aPKC RNAi in muscles, and SSR markers such as DLG and Scrib were not affected upon downregulating aPKC, Baz, and PTEN. It was suggested that either the F-actin/spectrin network might be responsible for the stabilization of GluRs, the spectrin-actin hexagonal lattice might serve as a framework that constrains the size of active zones and postsynaptic receptors, or that changes in GluR size and spacing could be a secondary consequence of the disruption of the SSR (Pielage et al., 2006). Our findings that the SSR in aPKC-RNAi-post and DLG distribution upon downregulating aPKC, Baz, and PTEN is not affected, but that GluR clusters are increased in size suggest that the size of GluR cluster is not necessarily dependent on the SSR or DLG. Together with the studies of Chen et al. (2006) demonstrating that disruption of F-actin does not alter the formation of GluRIIB-clusters, the results of Pielage et al (2006) and ours are consistent with the idea that the F-actin/spectrin network might restrict GluR- cluster size.

Downregulating aPKC, Baz, or PTEN levels in the muscle, besides decreasing postsynaptic F-actin localization, also result in a substantial increase in synaptic bouton size and a decrease in NMJ expansion. As the larval NMJ arbors are completely surrounded by the muscle membrane, NMJ expansion and bouton size are likely regulated by forces involving a balance between cytoskeletal extension at the presynaptic arbors and cytoskeletal retraction at the postsynaptic sites. Not surprisingly, interfering with this balance leads to misregulation of NMJ extension and bouton size. Interestingly, our previous studies suggest that aPKC might play different roles in the regulation of the presynaptic versus postsynaptic cytoskeletons. At the presynapse, aPKC is associated with microtubules and regulates microtubule stability through interactions with the presynaptic MAPB-related protein Futsch (Ruiz-Canada et al., 2004). In muscles, aPKC is also associated with microtubules, but regulates both postsynaptic F-actin/spectrin through Baz (this report) and postsynaptic microtubules (Ruiz-Canada et al., 2004). The exact mechanisms for the regulation of postsynaptic microtubules by aPKC are not known. This regulation might involve the modulation of an as yet unknown muscle microtubule-associated protein, or might result from indirect regulation by the stabilization of F-actin, which might exclude microtubules. In summary, our study reveals a novel mechanism by which the postsynaptic F-actin cytoskeleton is regulated during NMJ growth. In this mechanism F-actin organization at the postsynaptic region depends at least in part on Baz function. In turn, proper localization of Baz at this F-actin region depends on the opposing actions of aPKC and PTEN. The conservation of the aPKC-Baz-PTEN interaction across different cell types argues in favor of common mechanisms for cytoskeletal regulation by this complex in many tissues. Further, our studies establish a mechanism by which the dynamics of the postsynaptic actin cytoskeleton might be regulated during plasticity in the brain.

Supplementary Material

Refer to Web version on PubMed Central for supplementary material.

Acknowledgments

We would like to thank Dr. Sean Speese for helpful comments on the manuscript, and members of the Budnik laboratory for discussions. We also thank Dr. Ricardo Medina for helpful advice in the phosphorylation assays, and Drs. Daniel St. Johnston, Ronald Dubreil, Graeme Davis, Duojia Pan, and the Bloomington Stock Center for providing fruit fly stocks. This work was supported from NIH grant R01 NS030072 to V.B. Core resources supported by the Diabetes Endocrinology Research Center grant DK32520 were also used.

References

Alvarez VA, Sabatini BL. Anatomical and Physiological Plasticity of Dendritic Spines. Annu Rev Neurosci. 2007

Anholt RR, Mackay TF. Quantitative genetic analyses of complex behaviours in Drosophila. Nat Rev Genet. 2004; 5:838–849. [PubMed: 15520793]

Ashley J, Packard M, Ataman B, Budnik V. Fasciclin II signals new synapse formation through amyloid precursor protein and the scaffolding protein dX11/Mint. J Neurosci. 2005; 25:5943–5955. [PubMed: 15976083]

Benton R, St Johnston D. A conserved oligomerization domain in drosophila Bazooka/PAR-3 is important for apical localization and epithelial polarity. Curr Biol. 2003; 13:1330–1334. [PubMed: 12906794]

Benton R, St Johnston D. Drosophila PAR-1 and 14-3-3 inhibit Bazooka/PAR-3 to establish complementary cortical domains in polarized cells. Cell. 2003; 115:691–704. [PubMed: 14675534]

Budnik V, Koh YH, Guan B, Hartmann B, Hough C, Woods D, Gorczyca M. Regulation of synapse structure and function by the Drosophila tumor suppressor gene dlg. Neuron. 1996; 17:627–640. [PubMed: 8893021]

Cai XM, Tao BB, Wang LY, Liang YL, Jin JW, Yang Y, Hu YL, Zha XL. Protein phosphatase activity of PTEN inhibited the invasion of glioma cells with epidermal growth factor receptor mutation type III expression. Int J Cancer. 2005; 117:905–912. [PubMed: 15986432]

Chan JR, Jolicoeur C, Yamauchi J, Elliott J, Fawcett JP, Ng BK, Cayouette M. The polarity protein Par-3 directly interacts with p75NTR to regulate myelination. Science. 2006; 314:832–836. [PubMed: 17082460]

Chen K, Merino C, Sigrist SJ, Featherstone DE. The 4.1 protein coracle mediates subunit-selective anchoring of Drosophila glutamate receptors to the postsynaptic actin cytoskeleton. J Neurosci. 2005; 25:6667–6675. [PubMed: 16014728]

Chen X, Macara IG. Par-3 controls tight junction assembly through the Rac exchange factor Tiam1. Nat Cell Biol. 2005; 7:262–269. [PubMed: 15723052]

Chen X, Macara IG. Par-3 mediates the inhibition of LIM kinase 2 to regulate cofilin phosphorylation and tight junction assembly. J Cell Biol. 2006; 172:671–678. [PubMed: 16505165]

Cohen CM, Tyler JM, Branton D. Spectrin-actin associations studied by electron microscopy of shadowed preparations. Cell. 1980; 21:875–883. [PubMed: 6893681]

Conder R, Yu H, Zahedi B, Harden N. The serine/threonine kinase dPak is required for polarized assembly of F-actin bundles and apical-basal polarity in the Drosophila follicular epithelium. Dev Biol. 2007; 305:470–482. [PubMed: 17383630]

Cox DN, Seyfried SA, Jan LY, Jan YN. Bazooka and atypical protein kinase C are required to regulate oocyte differentiation in the Drosophila ovary. Proc Natl Acad Sci U S A. 2001; 98:14475–14480. [PubMed: 11734648]

Coyle IP, Koh YH, Lee WC, Slind J, Fergestad T, Littleton JT, Ganetzky B. Nervous wreck, an SH3 adaptor protein that interacts with Wsp, regulates synaptic growth in Drosophila. Neuron. 2004; 41:521–534. [PubMed: 14980202]

DiAntonio A, Petersen SA, Heckmann M, Goodman CS. Glutamate receptor expression regulates quantal size and quantal content at the Drosophila neuromuscular junction. J Neurosci. 1999; 19:3023–3032. [PubMed: 10191319]

Dillon C, Goda Y. The actin cytoskeleton: integrating form and function at the synapse. Annu Rev Neurosci. 2005; 28:25–55. [PubMed: 16029114]

Drier EA, Tello MK, Cowan M, Wu P, Blace N, Sacktor TC, Yin JC. Memory enhancement and formation by atypical PKM activity in Drosophila melanogaster. Nat Neurosci. 2002; 5:316–324. [PubMed: 11914720]

Dubreuil RR, Wang P, Dahl S, Lee J, Goldstein LS. Drosophila beta spectrin functions independently of alpha spectrin to polarize the Na, K ATPase in epithelial cells. J Cell Biol. 2000; 149:647–656. [PubMed: 10791978]

Eaton BA, Davis GW. LIM Kinase1 controls synaptic stability downstream of the type II BMP receptor. Neuron. 2005; 47:695–708. [PubMed: 16129399]

Featherstone DE, Davis WS, Dubreuil RR, Broadie K. Drosophila alpha- and beta-spectrin mutations disrupt presynaptic neurotransmitter release. J Neurosci. 2001; 21:4215–4224. [PubMed: 11404407]

Frank H, Althoen SC. Testing hypothesis about population means. Statistics: Concepts and Applications. 1994:434.

Fraser MM, Bayazitov IT, Zakharenko SS, Baker SJ. Phosphatase and tensin homolog, deleted on chromosome 10 deficiency in brain causes defects in synaptic structure, transmission and plasticity, and myelination abnormalities. Neuroscience. 2008; 151:476–488. [PubMed: 18082964]

Gao X, Neufeld TP, Pan D. Drosophila PTEN regulates cell growth and proliferation through PI3K-dependent and -independent pathways. Dev Biol. 2000; 221:404–418. [PubMed: 10790335]

Greenspan RJ. Chapter 5: Analyis of Mutations. Fly pushing: The Theory and Practice of Drosophila Genetics. 2006

Hirose T, Izumi Y, Nagashima Y, Tamai-Nagai Y, Kurihara H, Sakai T, Suzuki Y, Yamanaka T, Suzuki A, Mizuno K, Ohno S. Involvement of ASIP/PAR-3 in the promotion of epithelial tight junction formation. J Cell Sci. 2002; 115:2485–2495. [PubMed: 12045219]

Izumi Y, Hirose T, Tamai Y, Hirai S, Nagashima Y, Fujimoto T, Tabuse Y, Kemphues KJ, Ohno S. An atypical PKC directly associates and colocalizes at the epithelial tight junction with ASIP, a mammalian homologue of Caenorhabditis elegans polarity protein PAR-3. J Cell Biol. 1998; 143:95–106. [PubMed: 9763423]

Jan LY, Jan YN. L-glutamate as an excitatory transmitter at the Drosophila larval neuromuscular junction. J Physiol (Lond). 1976; 262:215–236. [PubMed: 186587]

Ji SP, Zhang Y, Van Cleemput J, Jiang W, Liao M, Li L, Wan Q, Backstrom JR, Zhang X. Disruption of PTEN coupling with 5-HT2C receptors suppresses behavioral responses induced by drugs of abuse. Nat Med. 2006; 12:324–329. [PubMed: 16474401]

Jia XX, Gorczyca M, Budnik V. Ultrastructure of neuromuscular junctions in Drosophila: comparison of wild type and mutants with increased excitability [published erratum appears in J Neurobiol 1994 Jul;25(7):893–5]. J Neurobiol. 1993; 24:1025–1044. [PubMed: 8409967]

Kalidas S, Smith DP. Novel genomic cDNA hybrids produce effective RNA interference in adult Drosophila. Neuron. 2002; 33:177–184. [PubMed: 11804566]

Kalil K, Dent EW. Touch and go: guidance cues signal to the growth cone cytoskeleton. Curr Opin Neurobiol. 2005; 15:521–526. [PubMed: 16143510]

Koch I, Schwarz H, Beuchle D, Goellner B, Langegger M, Aberle H. Drosophila ankyrin 2 is required for synaptic stability. Neuron. 2008; 58:210–222. [PubMed: 18439406]

Koh YH, Popova E, Thomas U, Griffith LC, Budnik V. Regulation of DLG localization at synapses by CaMKII-dependent phosphorylation. Cell. 1999; 98:353–363. [PubMed: 10458610]

Kwon CH, Luikart BW, Powell CM, Zhou J, Matheny SA, Zhang W, Li Y, Baker SJ, Parada LF. Pten regulates neuronal arborization and social interaction in mice. Neuron. 2006; 50:377–388. [PubMed: 16675393]

Lee JO, Yang H, Georgescu MM, Di Cristofano A, Maehama T, Shi Y, Dixon JE, Pandolfi P, Pavletich NP. Crystal structure of the PTEN tumor suppressor: implications for its phosphoinositide phosphatase activity and membrane association. Cell. 1999; 99:323–334. [PubMed: 10555148]

Lin D, Edwards AS, Fawcett JP, Mbamalu G, Scott JD, Pawson T. A mammalian PAR-3-PAR-6 complex implicated in Cdc42/Rac1 and aPKC signalling and cell polarity. Nat Cell Biol. 2000; 2:540–547. [PubMed: 10934475]

Lynch G, Rex CS, Gall CM. LTP consolidation: substrates, explanatory power, and functional significance. Neuropharmacology. 2007; 52:12–23. [PubMed: 16949110]

Marrus SB, Portman SL, Allen MJ, Moffat KG, DiAntonio A. Differential localization of glutamate receptor subunits at the Drosophila neuromuscular junction. J Neurosci. 2004; 24:1406–1415. [PubMed: 14960613]

Matsuzaki M, Honkura N, Ellis-Davies GC, Kasai H. Structural basis of long-term potentiation in single dendritic spines. Nature. 2004; 429:761–766. [PubMed: 15190253]

Meng Y, Zhang Y, Tregoubov V, Falls DL, Jia Z. Regulation of spine morphology and synaptic function by LIMK and the actin cytoskeleton. Rev Neurosci. 2003; 14:233–240. [PubMed: 14513866]

Munro EM. PAR proteins and the cytoskeleton: a marriage of equals. Curr Opin Cell Biol. 2006; 18:86–94. [PubMed: 16364625]

Nagai-Tamai Y, Mizuno K, Hirose T, Suzuki A, Ohno S. Regulated protein-protein interaction between aPKC and PAR-3 plays an essential role in the polarization of epithelial cells. Genes Cells. 2002; 7:1161–1171. [PubMed: 12390250]

Ning K, Pei L, Liao M, Liu B, Zhang Y, Jiang W, Mielke JG, Li L, Chen Y, El-Hayek YH, Fehlings MG, Zhang X, Liu F, Eubanks J, Wan Q. Dual neuroprotective signaling mediated by downregulating two distinct phosphatase activities of PTEN. J Neurosci. 2004; 24:4052–4060. [PubMed: 15102920]

Nishimura T, Yamaguchi T, Kato K, Yoshizawa M, Nabeshima Y, Ohno S, Hoshino M, Kaibuchi K. PAR-6-PAR-3 mediates Cdc42-induced Rac activation through the Rac GEFs STEF/Tiam1. Nat Cell Biol. 2005; 7:270–277. [PubMed: 15723051]

Nunes P, Haines N, Kuppuswamy V, Fleet DJ, Stewart BA. Synaptic vesicle mobility and presynaptic F-actin are disrupted in a N-ethylmaleimide-sensitive factor allele of Drosophila. Mol Biol Cell. 2006; 17:4709–4719. [PubMed: 16914524]

Ohno S. Intercellular junctions and cellular polarity: the PAR-aPKC complex, a conserved core cassette playing fundamental roles in cell polarity. Curr Opin Cell Biol. 2001; 13:641–648. [PubMed: 11544035]

Packard M, Koo ES, Gorczyca M, Sharpe J, Cumberledge S, Budnik V. The Drosophila wnt, wingless, provides an essential signal for pre- and postsynaptic differentiation. Cell. 2002; 111:319–330. [PubMed: 12419243]

Parnas D, Haghighi AP, Fetter RD, Kim SW, Goodman CS. Regulation of Postsynaptic Structure and Protein Localization by the Rho-Type Guanine Nucleotide Exchange Factor dPix. Neuron. 2001; 32:415–424. [PubMed: 11709153]

Pastalkova E, Serrano P, Pinkhasova D, Wallace E, Fenton AA, Sacktor TC. Storage of spatial information by the maintenance mechanism of LTP. Science. 2006; 313:1141–1144. [PubMed: 16931766]

Pawson C, Eaton BA, Davis GW. Formin-dependent synaptic growth: evidence that Dlar signals via Diaphanous to modulate synaptic actin and dynamic pioneer microtubules. J Neurosci. 2008; 28:11111–11123. [PubMed: 18971454]

Pielage J, Fetter RD, Davis GW. Presynaptic spectrin is essential for synapse stabilization. Curr Biol. 2005; 15:918–928. [PubMed: 15916948]

Pielage J, Fetter RD, Davis GW. A postsynaptic spectrin scaffold defines active zone size, spacing, and efficacy at the Drosophila neuromuscular junction. J Cell Biol. 2006; 175:491–503. [PubMed: 17088429]

Pinal N, Goberdhan DC, Collinson L, Fujita Y, Cox IM, Wilson C, Pichaud F. Regulated and polarized PtdIns(3,4,5)P3 accumulation is essential for apical membrane morphogenesis in photoreceptor epithelial cells. Curr Biol. 2006; 16:140–149. [PubMed: 16431366]

Prokop A. Organization of the efferent system and structure of neuromuscular junctions in Drosophila. Int Rev Neurobiol. 2006; 75:71–90. [PubMed: 17137924]

Roche JP, Packard MC, Moeckel-Cole S, Budnik V. Regulation of synaptic plasticity and synaptic vesicle dynamics by the PDZ protein Scribble. J Neurosci. 2002; 22:6471–6479. [PubMed: 12151526]

Ruiz-Canada C, Ashley J, Moeckel-Cole S, Drier E, Yin J, Budnik V. New Synaptic Bouton Formation Is Disrupted by Misregulation of Microtubule Stability in aPKC Mutants. Neuron. 2004; 42:567–580. [PubMed: 15157419]

Sato K, Hattori S, Irie S, Sorimachi H, Inomata M, Kawashima S. Degradation of fodrin by m-calpain in fibroblasts adhering to fibrillar collagen I gel. J Biochem. 2004; 136:777–785. [PubMed: 15671488]

Shi SH, Jan LY, Jan YN. Hippocampal neuronal polarity specified by spatially localized mPar3/mPar6 and PI 3-kinase activity. Cell. 2003; 112:63–75. [PubMed: 12526794]

Sone M, Hoshino M, Suzuki E, Kuroda S, Kaibuchi K, Nakagoshi H, Saigo K, Nabeshima Y, Hama C. Still life, a protein in synaptic terminals of Drosophila homologous to GDP-GTP exchangers. Science. 1997; 275:543–547. [PubMed: 8999801]

Stewart BA, Atwood HL, Renger JJ, Wang J, Wu C-F. Drosophila neuromuscular preparations in haemolymph-like physiological salines. J Comp Physiol (A). 1994; 175:179–191. [PubMed: 8071894]

Tada T, Sheng M. Molecular mechanisms of dendritic spine morphogenesis. Curr Opin Neurobiol. 2006; 16:95–101. [PubMed: 16361095]

Tamura M, Gu J, Matsumoto K, Aota S, Parsons R, Yamada KM. Inhibition of cell migration, spreading, and focal adhesions by tumor suppressor PTEN. Science. 1998; 280:1614–1617. [PubMed: 9616126]

Thomas U, Kim E, Kuhlendahl S, Koh YH, Gundelfinger ED, Sheng M, Garner CC, Budnik V. Synaptic clustering of the cell adhesion molecule fasciclin II by discs-large and its role in the regulation of presynaptic structure. Neuron. 1997; 19:787–799. [PubMed: 9354326]

Traweger A, Wiggin G, Taylor L, Tate SA, Metalnikov P, Pawson T. Protein phosphatase 1 regulates the phosphorylation state of the polarity scaffold Par-3. Proc Natl Acad Sci U S A. 2008; 105:10402–10407. [PubMed: 18641122]

von Stein W, Ramrath A, Grimm A, Muller-Borg M, Wodarz A. Direct association of Bazooka/PAR-3 with the lipid phosphatase PTEN reveals a link between the PAR/aPKC complex and phosphoinositide signaling. Development. 2005; 132:1675–1686. [PubMed: 15743877]

Wang Y, Cheng A, Mattson MP. The PTEN phosphatase is essential for long-term depression of hippocampal synapses. Neuromolecular Med. 2006; 8:329–336. [PubMed: 16775384]

Watts JL, Etemad-Moghadam B, Guo S, Boyd L, Draper BW, Mello CC, Priess JR, Kemphues KJ. par-6, a gene involved in the establishment of asymmetry in early C. elegans embryos, mediates the asymmetric localization of PAR-3. Development. 1996; 122:3133–3140. [PubMed: 8898226]

Wodarz A. Establishing cell polarity in development. Nat Cell Biol. 2002; 4:E39–44. [PubMed: 11835058]

Wodarz A, Ramrath A, Grimm A, Knust E. Drosophila atypical protein kinase C associates with Bazooka and controls polarity of epithelia and neuroblasts. J Cell Biol. 2000; 150:1361–1374. [PubMed: 10995441]

Wu H, Feng W, Chen J, Chan LN, Huang S, Zhang M. PDZ domains of Par-3 as potential phosphoinositide signaling integrators. Mol Cell. 2007; 28:886–898. [PubMed: 18082612]

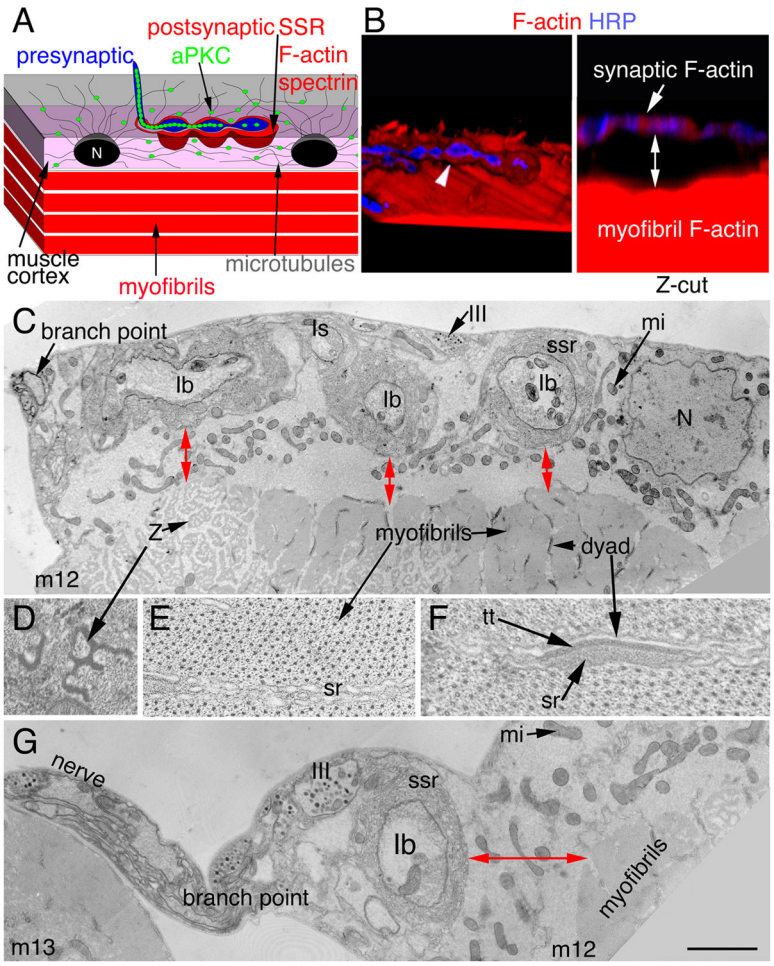

Figure 1. Arrangement of postsynaptic F-actin and the SSR in relationship to the contractile apparatus

(**A**) Diagram of the NMJ showing the relative positions of post-synaptic F-actin/spectrin, aPKC, microtubules, the SSR and the contractile apparatus. N= nucleus.

(**B**) 3-D rendered confocal images of a wild type arbor at muscle 12 labeled with anti-HRP (blue) and rhodamine-phalloidin (red) in (**left panel**; also see Suppl. Movie 1) a X-Y-Z 3-D isosurface rendering showing a single NMJ branch containing synaptic boutons (blue) surrounded by postsynaptic F-actin-rich domain (red) sitting above the contractile apparatus (red) of the muscle. In the **right panel**, the same image is now shown in a Y–Z plane, demonstrating that postsynaptic F-actin (red) surrounding synaptic boutons (blue) appears separate from the F-actin at the contractile apparatus (distance marked by a two-way arrow). Arrow and arrowhead point to the postsynaptic actin.

(**C**) Transmission electron micrograph through an NMJ branch at muscle 12 (m12) showing several boutons (Ib, Is, III) and a region of the contractile apparatus near the NMJ branch-point. Red two-way arrows show the distance between the SSR and the myofibrils of the contractile apparatus in these hypercontractile muscles.

(**D–F**) High magnification views of myofibril regions showing (**D**) perforated Z-bands, (**E**) the myosin-actin lattice and the sarcoplasmic reticulum (sr), and (**F**) the dyads composed of the t-tubule (tt) and sr compartments.

(**G**) View of the nerve as it runs from muscle 13 (m13) to muscle 12 and the NMJ branch-point at muscle 12. At this region the distance between the SSR and muscle contractile

apparatus (two-way arrow) is larger. N= nucleus; Z= perforated Z band; mi =mitochondria; ssr= subsynaptic reticulum.
Calibration bar is 3.5 μm in B, 0.4 μm in C, G and 80 nm in D–F.

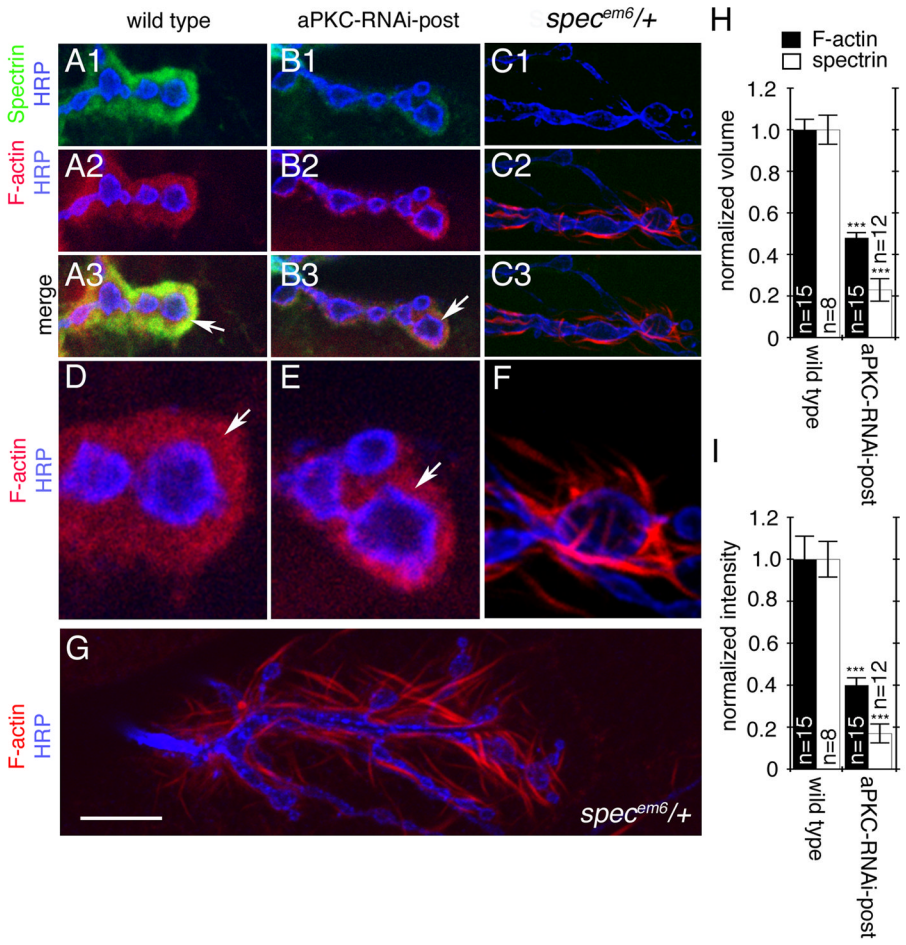

Figure 2. Localization of Spectrin and F-actin at NMJs of wild type, aPKC RNAi-post, and *β-spec^em6/+* mutants

(**A, B,C**) Single confocal slices of third instar NMJ branches at muscles12/13 in preparations, triple stained with anti-HRP (blue), anti-α-spectrin (green), and rhodamine-phalloidin (red) in (**A**), wild type, (**B**) larvae expressing aPKC-RNAi in muscles, (**C**) *β-spec^em6/+* mutants.

(**D, E, F**) are high magnification views of synaptic boutons in the above genotypes stained with anti-HRP (blue) and rhodamine-phalloidin (red) showing the distribution of F-actin around the presynaptic compartment labeled by anti-HRP.

(**G**) Extended view of an NMJ at muscle 12/13 in a *β-spec^em6/+* heterozygote larval body wall muscle preparation stained with anti-HRP (blue) and rhodamine-phalloidin (red) showing the organization of F-actin into wisps/spikes. Arrows point to the F-actin-rich postsynaptic area.

(**H, I**) Quantification of the (**H**) normalized volume and (**I**) normalized fluorescence intensityof postsynaptic α-spectrin (white bars) and F-actin (black bars) in the indicated genotypes. Data was normalized to wild type controls. “n” represents number of boutons. Calibration bar is 7 μm for A, B, C, 2 μm for D, E, F, and 10 μm for G.

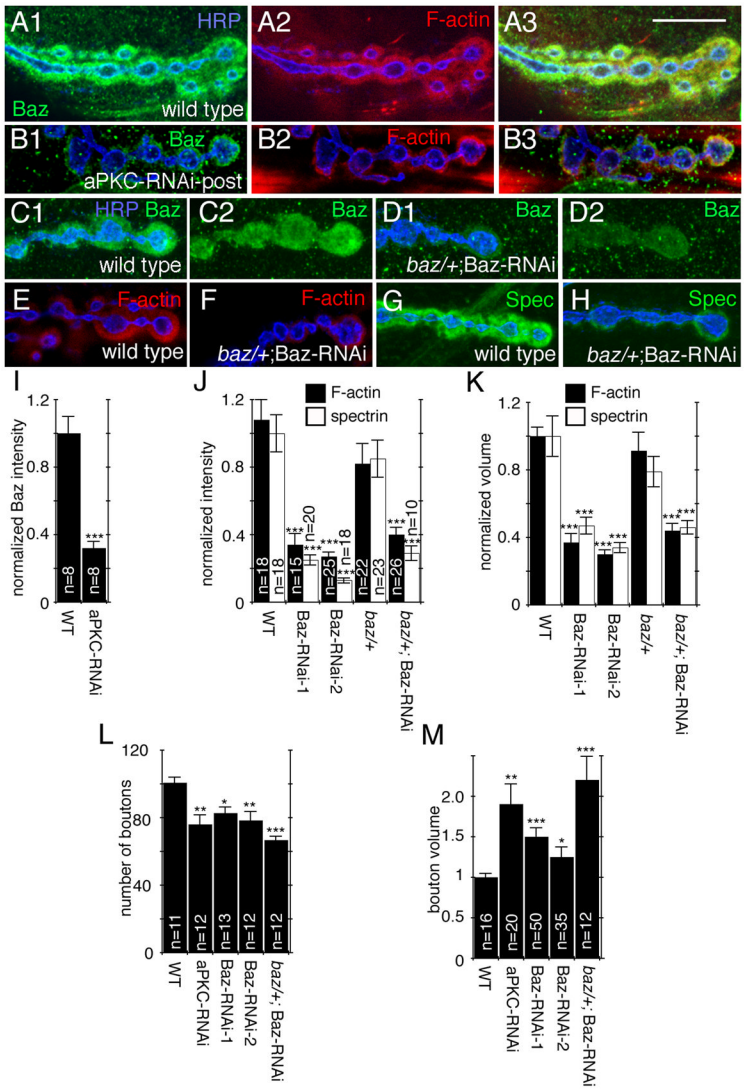

Figure 3. Baz is enriched in the F-actin region and reduction in Baz levels phenocopy aPKC downregulation at the NMJ

Single confocal slices of third instar larval NMJs,

(**A–B**) Triple stained with anti-HRP (blue), anti-Baz (green) and rhodamine-phalloidin (red) in **(A)** wild type or **(B)** aPKC-RNAi-Post (muscle 12).

(**C–D**) Double stained with anti-HRP (blue) and anti-Baz (green) in **(C)** wild type and **(D)** *baz*/+; Baz RNAi-post (muscle 6 or 7).

(E–H) Double stained with anti-HRP (blue) and **(E–F)** rhodamine-phalloidin (red), or **(G–H)** anti-α-spectrin (green) in (**E,G)** wild type (**F, H**) *baz*/+; Baz RNAi-post (muscles 12/13 for F-actin and mudcles 6/7 for spectrin)

(**I–M**) Quantification of (**I**) normalized postsynaptic Baz intensity (“n” represents number of boutons”, (**J**) normalized postsynaptic F-actin (black bars, muscles 12/13), and spectrin (white bars, muscles 6/7) intensity (“n” represents number of boutons), **(K)** normalized postsynaptic volume (n is the same as in J), (**L**) bouton number (n represents number of arbors), and (**M**) bouton volume (n represents number of boutons) in the indicated genotypes.

Calibration bar is 15 μm for A, B, and 10 μm for C–H.

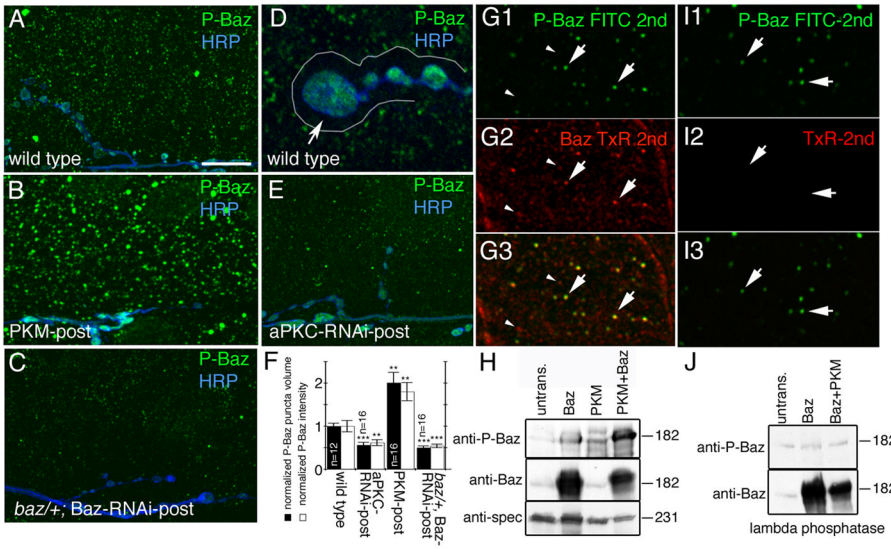

Figure 4. Baz is phosphorylated by aPKC in muscles and is absent from the postsynaptic F-actin-rich area

(**A–E**) Third instar muscle regions and NMJs at muscles 6 or 7 in preparations labeled with anti-phospho Baz (green) and anti-HRP (blue) in (**A, D**) wild type, (**B**) PKM-post, (**C**) *baz/+;* Baz-RNAi-post and (**E**) aPKC-RNAi-post. Arrow in **D** points to the postsynaptic F-actin rich area outlined by a white line, which is devoid of phospho-Baz.

(**F**) Quantification of the volume and intensity of phospho-Baz puncta in muscles of wild type, aPKC-RNAi-post, and PKM-post. Data was normalized to wild type values (n represents number of muscles).

(**G, I**) Confocal image of a muscle region in a preparation (**G**) sequentially labeled with antibodies to P-Baz (green) and Baz (red) showing that each P-Baz puncta colocalizes to a Baz puncta (arrows), and that only a subset of Baz puncta contains phosphorylated P-Baz (arrowheads point to Baz puncta devoid of P-Baz immunoreactivity), and (**I**) treated similar to G, but in an experiment were the anti-Baz antibody was omitted to ensure that the first secondary antibody (FITC 2nd) saturated all anti-P-Baz sites, which is observed in I2 by the lack of signal upon incubation with the TxR-2nd antibody.

(**H, J**) Western blots of S2 cell extracts transfected with the constructs indicated above the blots and probed sequentially with the antibodies indicated at the left, showing (**H**) the phosphorylation of Baz by PKM and (**J**) the lambda phosphatase assay. Untrans=untransfected cells.

Calibration bar is 14 μm for A, B, C, E, 5 μm for D, and 2 μm for G.

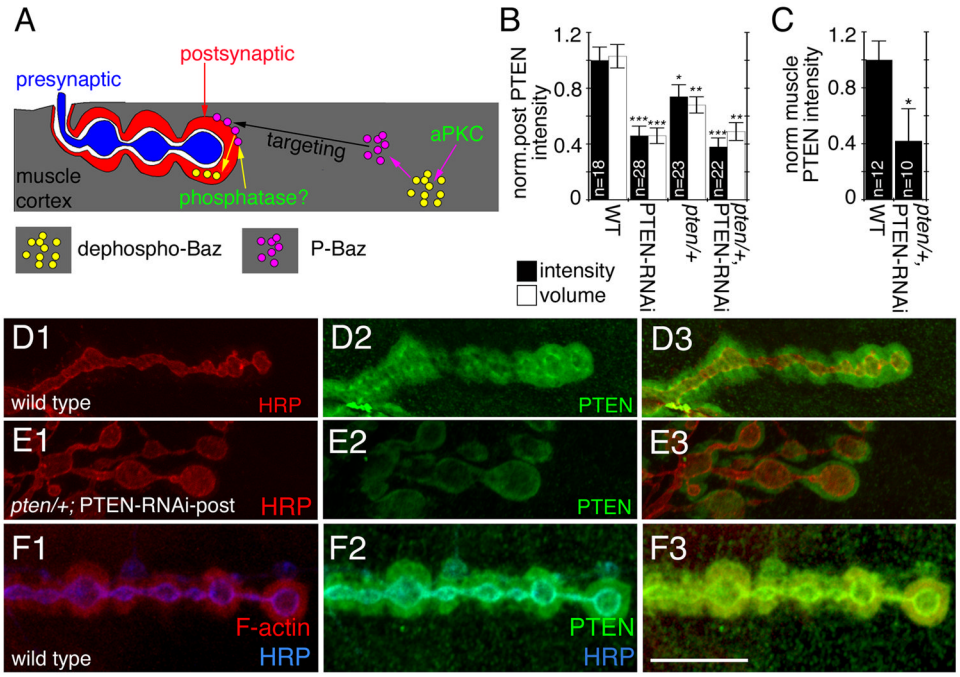

Figure 5. PTEN is localized at the postsynaptic F-actin-rich area

(**A**) A model of Baz trafficking at the NMJ. See text for details.

(**B–C**) Quantification of **(B)** normalized postsynaptic PTEN fluorescence intensity (black bars) and normalized volume (white bars) in the indicated genotypes (n represents number of boutons) and **(C)** normalized cortical PTEN intensity in the indicated genotypes (n represents number of muscles).

(**D–E**) Third instar NMJs at muscles 6 or 7 in preparation double stained with anti-PTEN (green) and anti-HRP (red) in **(D)** wild type and **(E)** *pten/+*; PTEN-RNAi-post.

(F) Third instar NMJ from wild type triple labeled with rhodamine-phalloidin (red), anti-PTEN (green) and anti-HRP (blue).

Calibration bar is 14 μm for D–F.

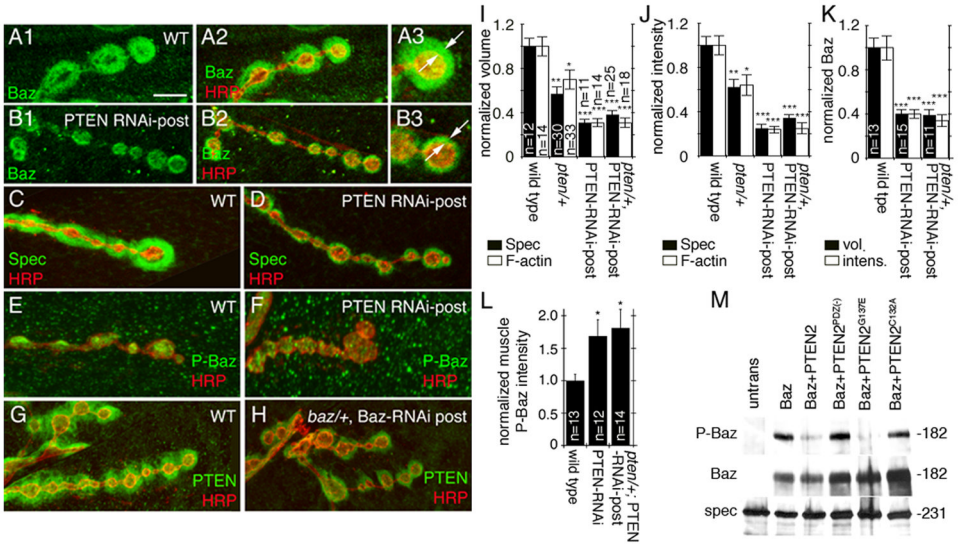

Figure 6. PTEN induces dephosphorylation of Bazooka and affects the postsynaptic actin spectrin area

(**A–B**) Third instar NMJs at muscles 6 or 7 double stained with anti-HRP (red) and anti-Baz (green) in (**A)** wild type, (**B)** PTEN-RNAi-post. Note the reduction in postsynaptic Baz in PTEN-RNAi-post compared to the wild type as indicated by arrows in A3, B3.

(C–F) Third instar NMJs stained with anti-HRP (red) and either **(C,D)** anti-α-spectrin (green), or **(E,F)** anti-phospho-Baz (green) in **(C,E)** wild type and **(D,F)** PTEN-RNAi-Post.

(G–H) Third instar NMJs stained with anti-HRP (red) and anti-PTEN (green) in **(G)** wild type and (**H**) *baz/+*; Baz-RNAi-post.

(**I, J**) Quantification of (**I**) normalized volume and (**J**) normalized intensity of α-spectrin (black bars; muscles 6 or 7) and F-actin (white bars, muscle 12) in the indicated genotypes. n represents number of boutons, and n is the same for I and J.

(**K**) Quantification of normalized postsynaptic Baz volume (black bars) and normalized postsynaptic Baz fluorescence intensity (white bars) in the indicated genotypes. n represents number of boutons.

(L) Quantification of normalized phospho-Baz fluorescence intensity in wild type, PTEN RNAi-post and *pten/+;* PTEN RNAi-post. n represents number of muscles.

(**M**) Western blot of S2 cell extracts from cells transfected with the genes shown above the blots and probed sequentially with the antibodies indicated at the left, showing the dephosphorylation of Baz by PTEN.

Calibration bar is 7μm for A1–2, B1–2, C–H and 3.5 μm for A3, B3.

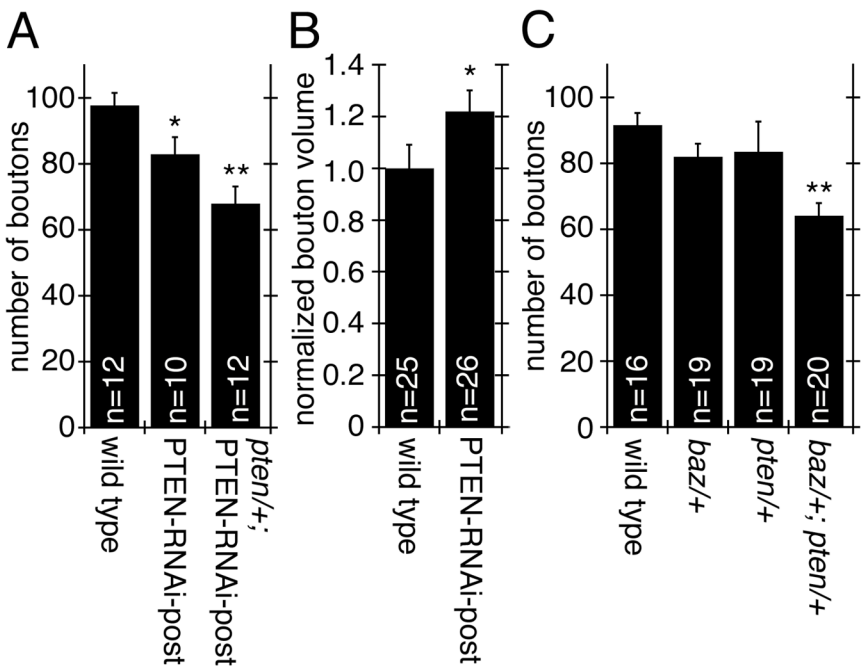

Figure 7. Downregulation of PTEN affects bouton number and bouton volume

(A–C) Quantification of **(A, C)** bouton number in the indicated genoptyes (n represents number of arbors), and **(B)** normalized bouton volume (n represents number of boutons).

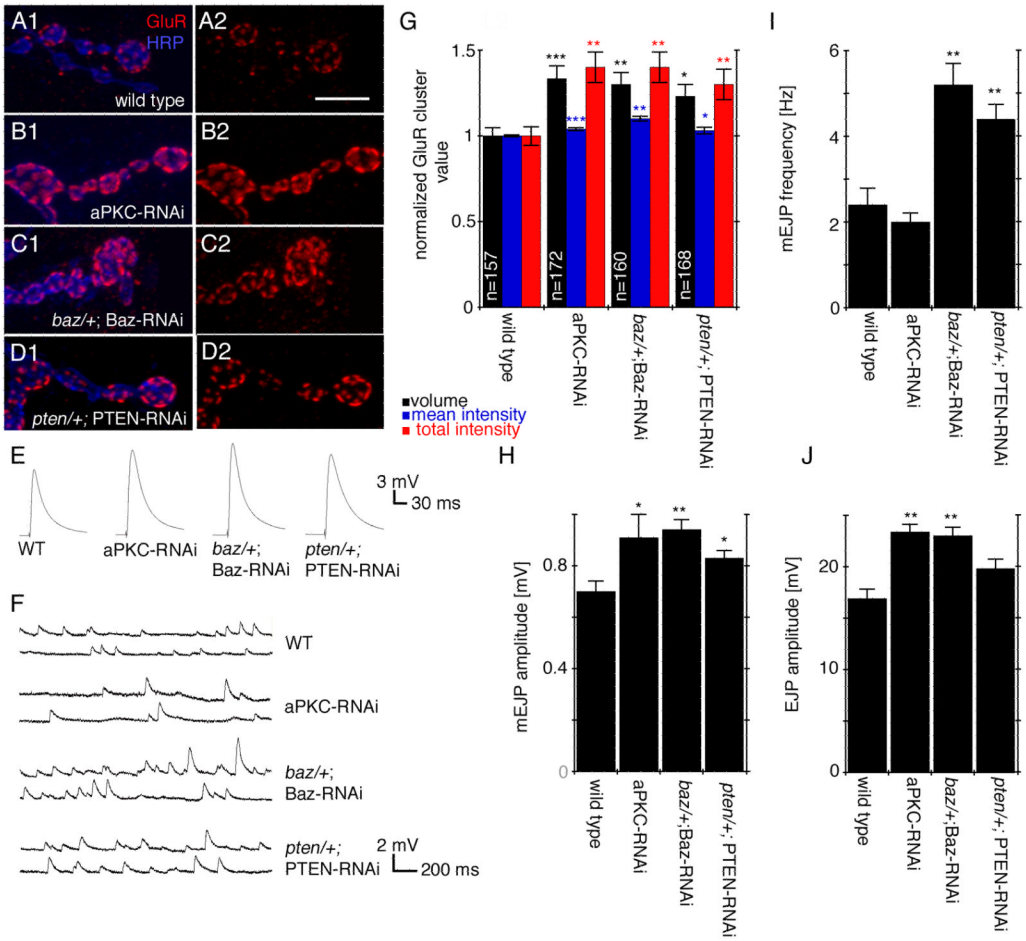

Figure 8. Downregulation of aPKC, PTEN and Baz have similar effects on synaptic transmission and glutamate receptor localization

(**A–D**) Third instar larval NMJs labeled with HRP (blue) and GluRIIA (red) in (**A**) wild type, (**B**) aPKCs-RNAi-post, (**C**) *baz/+;* Baz-RNAi-post, and (**D**) *pten/+;* PTEN-RNAi-post.

(**E, F**) Electrophysiological traces of (**E**) EJPs and (**F**) mEJPs in the indicated genotypes.

(**G, H, I, J**) Quantification of (**G**) GluRIIA cluster volume (black bars), mean intensity (blue bars), and total intensity (red bars) (n represents number of clusters), (**H**) mEJP amplitude, (**I**) mini EJP frequency, and (**K**) EJP amplitude in the indicated genotypes. In (**H**–**J**) n=6 animals for all genotypes.

Calibration bar is 7 μm for A–D.

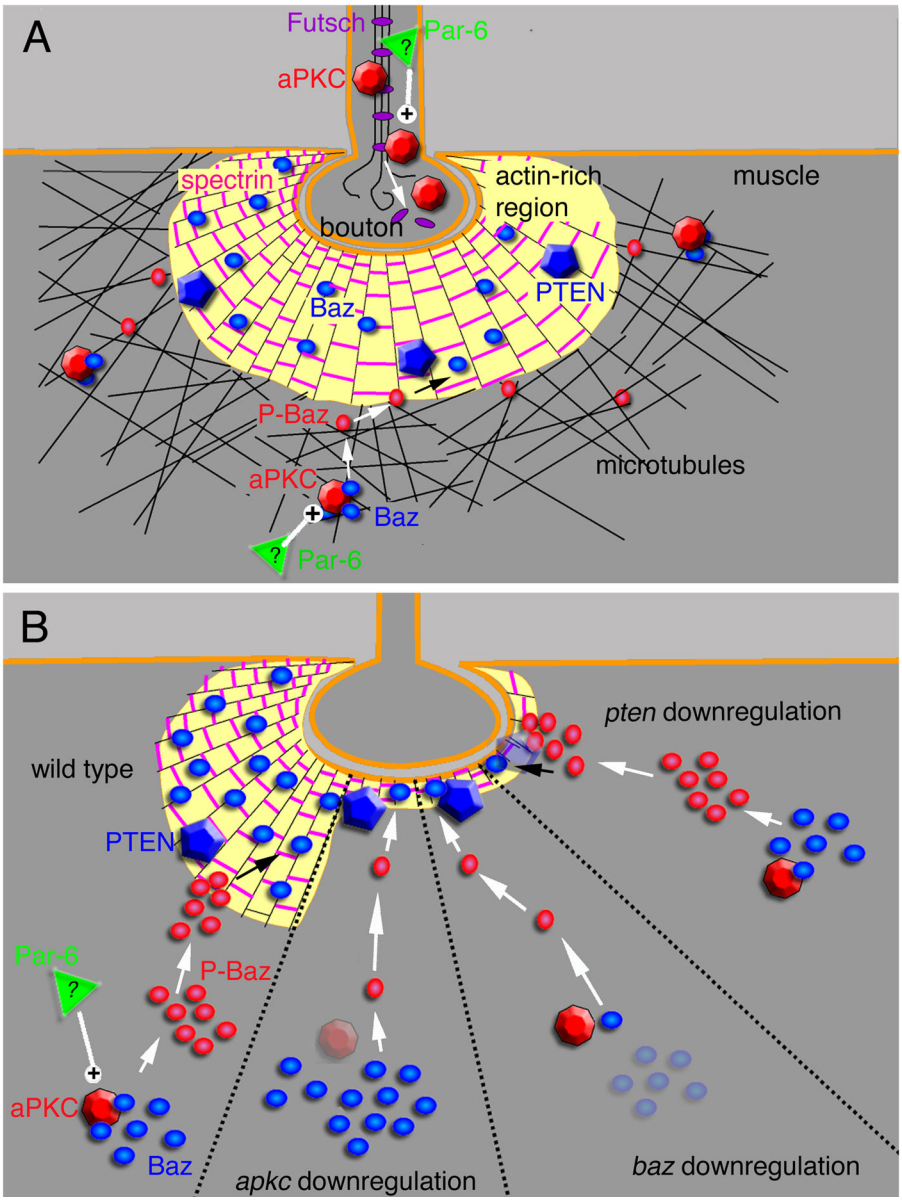

Figure 9. Proposed model for the regulation of the synaptic cytoskeleton by the aPKC-Baz-Par-6 complex at the larval NMJ

(A) At the presynaptic compartment, aPKC regulates microtubule stability by facilitating an interaction between the MAP1B-related Futsch and bundled microtubules (see (Ruiz-Canada et al., 2004)). At the postsynaptic compartment, aPKC regulates both F-actin and microtubules (Ruiz-Canada et al., 2004). Here we propose that the regulation of the F-actin cytoskeleton is carried out through the opposing functions of aPKC and PTEN by modulating the phosphorylation state of Baz (see text for details).

In (**B**) the synaptic bouton has been subdivided into 4 regions, each representing a different genotype as indicated, and the consequence of each genotype on the F-actin-rich postsynaptic region (see text for details).